

RADIATION EFFECT ON MAGNETOHYDRODYNAMIC CARREAU NANOFUID FLOW PAST NON-LINEAR PERMEABLE HEATED STRETCHING SHEET WITH PARTIAL SLIP

Hameda M. Shawky ^(a), Nabil T. M. Eldabe ^(b), Kawther A. Kamel and Esmat A. Abd-Aziz ^(a)

^(a) Department of Mathematics, Faculty of Science, Al-Azhar University.

^(b) Department of Mathematics, Faculty of Education, Ain Shams University.

*Corresponding Author: e-mail:osama_96348@yahoo.com

ABSTRACT

The motion of a Carreau nanofluid past an infinite vertical non-linear permeable stretching sheet embedded in a non-Darcy porous medium is investigated. It is stressed by a uniform external magnetic field. The thermal radiation and heat generation are taken in consideration as well as Brownian motion with thermophoresis, chemical reaction and partial slip velocity at the boundary layer. The nonlinear partial differential equations describing the motion with heat and mass transfer are transformed to non-linear ordinary differential equations and solved by using Runge-Kutta method with appropriate boundary conditions. The effects of the physical parameters of the problem on the obtained solutions are discussed numerically and graphically. Through the section of discussion the skin friction and the rate of heat and mass transfer are computed. It is found that these physical parameters play an important rules to control the obtained velocity, temperature and concentration of the fluid.

Keywords: Carreau nanofluid, partial slip: Non-Newtonian, magnetohydrodynamic, Radiation.

Nomenclature

D_B, D_T	Brownian , thermophoretic diffusion coefficients	N_b	Brownian motion parameter
λ	buoyancy parameter	β_T, β_c	coefficient of volumetric thermal and concentration
C	concentration	h	convective heat transfer coefficient
N, N_1	constant of proportionality	D_u	Dufour number
f	dimensionless stream function	θ	dimensionless temperature
ρ_p	Density of nano-particles	σ	electrical conductivity
E_c	Eckert number	ρ_f	fluid density
F_S	Forcheimmer number	Q	heat generation
$(\rho C)_p, (\rho C)_f$	heat capacities of nano particles and fluid	Da^{-1}	inverse Darcy number
ν	kinematic viscosity of fluid	$\nu = \frac{\mu f}{\rho_f}$	kinematic viscosity of the fluid
L_e	Lewis number	Re_x	local Reynolds number
G_m	local concentration Grashof number	G_r	local thermal Grashof number
M	Magnetic parameter for nanoparticles	k_e	mean absorption coefficient

k	nano-thermal conductivity	b_1	non-darcian coefficient
ϕ	nanoparticle volume fraction	Nu	Nusselt number
W_e	non-Newtonian Weissenberg parameter	k_0	permeability of the medium
n	power law index	P_r	Prandtl number
R	radiation parameter	C_f	skin-friction coefficient
$\tau = (\rho C)_p / (\rho C)_f$	ratio between heat capacity of the nano-particles with fluid	Sh	Sherwood number
B_0	strength of the magnetic field	v_w	suction/injection
$a > 0$	stretching parameter	σ_s	Stephen Boltzman constant
u_s	slip velocity	l	slip length
m	stretching index	δ	solatal buoyancy parameter
S_c	Schmidt number	T	temperature
$\Gamma > 0$	time constant	$a = k / (\rho c)_f$	thermal diffusivity parameter
T_f	temperature of hot fluid	N_t	thermophoresis parameter
T_w, C_w	Temperature, concentration at the wall	T_∞, C_∞	temperature, concentration at infinity
μ_f	viscosity of the zero shear rate	u, v	velocity components

Introduction

Nano fluid is the combination of simple fluid and nano sized particles uniformly suspended in the fluid. These nano sized particles can be metallic (Cu, Al, Hg, Ti, etc.) or non-metallic (Zno, Al_2O_3 , TiO_2 and several other metallic oxides). Nano particles have advantage over micro size particles due to negligible effects of gravitational setting and cluster formation during flow. Fluids are widely used in heat transfer phenomenon due to their strong convection properties. Nano fluids got the attention of researchers and industrialists due to their better performance in heat transfer phenomenon. Several researchers (Bang and Chang [1]; Suganthi and Rajan [2]; Kuznetsov [3]) have discussed the Nano fluid flow for various physical phenomenon by considering water as base fluid. But suspension of solid particles in water up to large percentage of its volume will change it from the

Newtonian to non-Newtonian fluid. Also we know that several non-Newtonian fluids have better heat transfer properties as compared with water for e.g. liquid metals. So it's important to discuss the flow of non-Newtonian nano fluids due to their wide range use in industrial and chemical processes. Choi [4] was the first one to use the term nano fluid due to nano sized particle suspension in fluid. He discussed that nano particles (due to their small size) are much better as compared to micro sized particles and their incorporation can reduce the cooling cost several times. Masuda et al [5] discussed the thermal conductivity enhancement due to addition of ultrafine Particles in fluid. Also Magnetohydro-dynamic non-Newtonian nanofluid flow over a stretching sheet through a non-Darcy porous medium with radiation and chemical reaction is discussed by El-Dabe, et al [6]. Awais M, et al [7] have been studied the velocity, thermal and concentration slip effects on a magneto-

hydrodynamic nanofluid flow. and El-dabe, et al [8] investigated the Magnetohydrodynamic peristaltic flow of Jeffry nanofluid with heat transfer through a porous medium in a vertical tube.

In many practical situations, the stretching surface does not need to be linear, e.g., in plastic sheet stretching. The heat transfer analysis of boundary layer flow over a continuous stretching surface with prescribed temperature or heat flux has gained considerable attention due to its applications in manufacture processes of polymer sheets, glass fiber, paper production, metal wires, plastic films, etc. In polymer, the glass and plastic industry quality of the final product greatly depends on the rate of cooling. Sakiadis [9] was the first to study the boundary layer flow over a continuous stretching surface. He developed the two dimensional boundary equations. Tsou et al. [10] examined the heat transfer effects on the boundary layer flow over a stretching surface. Erickson et al. [11] extended this work for mass transfer by considering suction and injection. Later on, many researchers have given their insight into boundary layer flows over linear stretching surfaces [12-14]. El-Dabe et. al. [15] investigated the effects of chemical reaction and heat radiation on the MHD flow of viscoelastic fluid through a porous medium over a horizontal stretching flat plate. The heat and mass transfer of MHD unsteady Maxwell fluid flow through porous medium past a porous flat plate is studied by El-Dabe et. al. [16]. Boundary layer flow of a nanofluid past a stretching sheet examined by Khan, et. Al [17]. Vishnu Ganesh, et. Al [18] have been studied the MHD radiative boundary layer flow of nanofluid past a vertical plate with internal heat generation/absorption, viscous and ohmic dissipation effects. Magnetohydrodynamic boundary layer heat transfer to a stretching sheet including viscous dissipation and internal heat generation in a porous medium discussed by Abou-zeid, Mohamed [19].

The main aim of this work is to discuss the effects of Dufour, Soret, thermal radiation,

chemical reaction, heat generation, viscous and ohmic dissipations on the boundary layer motion of an electrically conducting Carreau nanofluid past an infinite vertical heated stretching surface. The motion is stressed by a uniform external magnetic field as was as the effects of Brownian motion and thermophoresis. The system of non-linear partial differential equations describe the fluid motion is transformed to an ordinary differential equations by using a similarity transformations, then solved numerically by using Runge-Kutta method with shooting technique subjected to the appropriate boundary conditions. The effects of the physical parameters of the fluid on the obtained solutions are discussed numerically and illustrated graphically through set of figures.

Formulate of the problem:-

The flow of non-Newtonian nonfluid in the boundary layer past a stretching sheet is considered. By using the Cartesian coordinates (x , y), where x direction is taken along the vertical sheet and y-axis perpendicular to it as seen in Figure (1). The surface is stretched by a velocity $u_w = ax^m$. The components of the applied magnetic field are (0, B, 0). The induced magnetic field is negligible, when the assumption of small magnetic Reynolds number is considered. Also, electric field and the polarization are ignored.

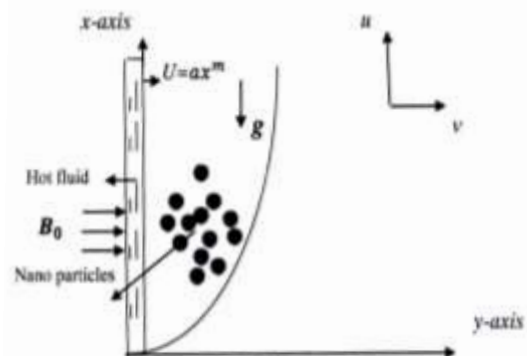


Fig. 1 Problem geometry

Carreau fluid model constitutive equation is defined as:

$$\tau_{ij} = \mu_f \left[1 + \frac{(n-1)}{2} (\Gamma \dot{\gamma})^2 \right] \dot{\gamma}_{ij}$$

In above equations τ_{ij} is the extra stress tensor and $\dot{\gamma}$ is defined as follows

$$\dot{\gamma} = \sqrt{\frac{1}{2} \sum_i \sum_j \dot{\gamma}_{ij} \dot{\gamma}_{ij}} = \sqrt{\frac{1}{2} \Pi} \quad (2)$$

Here Π is the second invariant strain tensor, in Cartesian coordinates we can write:

$$\dot{\gamma}_{11} = 2 \frac{\partial u}{\partial x}, \quad \dot{\gamma}_{12} = \dot{\gamma}_{21} = \frac{\partial u}{\partial y} + \frac{\partial v}{\partial x}, \quad \dot{\gamma}_{22} = 2 \frac{\partial v}{\partial y}. \quad (3)$$

Employing the Oberbeck-Boussinesq approximation, the governing equations of the flow field in steady state in Cartesian coordinates can be written in the dimensional form as

$$\frac{\partial u}{\partial x} + \frac{\partial v}{\partial y} = 0, \quad (4)$$

$$\rho_f \left(u \frac{\partial u}{\partial x} + v \frac{\partial u}{\partial y} \right) = \mu_f \frac{\partial^2 u}{\partial y^2} + \mu_f \frac{3(n-1)\Gamma^2}{2} \left(\frac{\partial u}{\partial y} \right)^2 \frac{\partial^2 u}{\partial y^2} + [(1 - C_\infty) \rho_{f\infty} \beta_T (T - T_\infty) - (\rho_p - \rho_{f\infty}) \beta_C (C - C_\infty)] g - \sigma B^2 u - \frac{\mu_f}{k_0} u - \frac{b_1}{k_0} u^2. \quad (5)$$

$$u \frac{\partial T}{\partial x} + v \frac{\partial T}{\partial y} = \alpha \frac{\partial^2 T}{\partial y^2} + \tau \left\{ D_B \left(\frac{\partial T}{\partial y} \frac{\partial C}{\partial y} \right) + \frac{D_T}{T_\infty} \left(\frac{\partial T}{\partial y} \right)^2 \right\} + \frac{\mu_f}{(\rho c_p)_f} \left(\frac{\partial u}{\partial y} \right)^2 + \frac{(n-1)\Gamma^2}{2} \frac{\mu_f}{(\rho c_p)_f} \left(\frac{\partial u}{\partial y} \right)^4 + \left(\frac{\sigma B_0^2}{\rho c_p} \right) u^2 + \frac{Q_0}{(\rho c_p)_f} (T - T_\infty) - \frac{1}{(\rho c_p)_f} \frac{\partial q_r}{\partial y} + \frac{D_m K_T}{c_s (\rho c_p)_f} \left(\frac{\partial^2 C}{\partial y^2} \right), \quad (6)$$

$$u \frac{\partial C}{\partial x} + v \frac{\partial C}{\partial y} = D_B \frac{\partial^2 C}{\partial y^2} + \left(\frac{D_T}{T_\infty} + \frac{D_m K_T}{T_m} \right) \frac{\partial^2 T}{\partial y^2} - K(C - C_\infty). \quad (7)$$

Magnetic field is chosen such that $B(x) = B_0 \sqrt{x^{m-1}}$

The subject appropriate boundary conditions are:-

$$u = u_w + u_s, \quad v = \pm v_w, \quad -k \frac{\partial T}{\partial y} = h(T_f - T), \quad C = C_w \quad \text{at } y = 0, \quad (8)$$

$$u \rightarrow 0; \quad T \rightarrow T_\infty; \quad C \rightarrow C_\infty \quad \text{as } y \rightarrow \infty$$

The slip velocity u_s , defined as:

$$u_s = l \left. \frac{\partial u}{\partial y} \right|_{y=0}, \quad \text{while } u_w = ax^m \quad (9)$$

In equation (6) the term of radiation can be takes the form

$$\frac{\partial q_r}{\partial y} = - \frac{16 \sigma_s T_\infty^3}{3k_e} \frac{\partial^2 T}{\partial y^2} \quad (10)$$

Invoking equation (10), equation (6) gets modified as

$$u \frac{\partial T}{\partial x} + v \frac{\partial T}{\partial y} = \left(\alpha + \frac{16 \sigma_s T_\infty^3}{3k_e (\rho c_p)_f} \right) \frac{\partial^2 T}{\partial y^2} + \tau \left\{ D_B \left(\frac{\partial T}{\partial y} \frac{\partial C}{\partial y} \right) + \frac{D_T}{T_\infty} \left(\frac{\partial T}{\partial y} \right)^2 \right\} + \frac{\mu_f}{(\rho c_p)_f} \left(\frac{\partial u}{\partial y} \right)^2 + \frac{(n-1)\Gamma^2}{2} \frac{\mu_f}{(\rho c_p)_f} \left(\frac{\partial u}{\partial y} \right)^4 + \left(\frac{\sigma B_0^2}{\rho c_p} \right) u^2 + \frac{Q_0}{(\rho c_p)_f} (T - T_\infty) + \frac{D_m K_T}{c_s (\rho c_p)_f} \left(\frac{\partial^2 C}{\partial y^2} \right). \quad (11)$$

Consider stream function = $\psi(x, y)$:-

$$u = \frac{\partial \psi}{\partial y}, \quad v = -\frac{\partial \psi}{\partial x}$$

Introducing following similarity transformations in the above equations, where

$$\left. \begin{aligned} \psi &= \sqrt{\frac{2\nu ax^{m+1}}{m+1}} f(\eta), & \theta &= \frac{T-T_\infty}{T_w-T_\infty}, & \phi &= \frac{C-C_\infty}{C_w-C_\infty} \\ u &= ax^m f'(\eta), & v &= -\sqrt{\frac{a(m+1)\nu x^{m-1}}{2}} \left[f(\eta) + \frac{m-1}{m+1} \eta f'(\eta) \right], & \eta &= \sqrt{\frac{a(m+1)x^{m-1}}{2\nu}} y. \\ Nr &= \frac{k_w k}{4\sigma_s T_\infty^3}, & R &= \frac{4}{3Nr}, & \lambda &= \frac{Gr}{Re_x^{\frac{1}{2}}}, & \delta &= \frac{Gm}{Re_x^{\frac{1}{2}}}. \\ Pr &= \frac{\nu}{\alpha}, & Sc &= \frac{\nu}{D_B}, & Nb &= \frac{\tau D_B}{\nu} (C_w - C_\infty), & Nt &= \frac{\tau D_T}{\nu T_\infty} (T_w - T_\infty). \\ Re_x &= \frac{U_w(x)x}{\nu}, & Gr &= \frac{(1-C_\infty) \left(\frac{\rho f_\infty}{\rho_f} \right) g n (T_w - T_\infty)}{\nu^2 Re_x^{\frac{1}{2}}}, & Gm &= \frac{\left(\frac{\rho_f - \rho f_\infty}{\rho_f} \right) g n_1 (C_w - C_\infty)}{\nu^2 Re_x^{\frac{1}{2}}}. \\ We &= \Gamma \sqrt{\frac{a^3(m+1)x^{3m-1}}{2\nu}}, & M^2 &= \frac{\sigma B_0^2}{\rho_f a}, & Q &= \frac{Q_0}{\rho_f a c_p}, & Du &= \frac{D_m k_T (C_w - C_\infty)}{C_s c_p \nu (T_w - T_\infty)}. \\ S_r &= \frac{D_m k_T (T_w - T_\infty)}{T_\infty \nu (C_w - C_\infty)}, & Ec &= \frac{u_w^2}{c_p (T_w - T_\infty)}, & Da^{-1} &= \frac{\nu}{a k_0}, & F_s &= \frac{a b_1}{u_w}. \end{aligned} \right\} \quad (12)$$

In view of the above similarity, the equations (5, 7 and 11) reduce to

$$f'''' + ff'' - \frac{2}{m+1} \left(m + \frac{F_s Re}{Da} \right) f'^2 + \frac{3(n-1)}{2} We^2 (f''')^2 f'''' + \frac{2}{m+1} (\lambda\theta - \delta\phi) - \left(\frac{2}{m+1} M^2 + \frac{1}{Da Re_{m,x}} \right) f' = 0. \quad (13)$$

$$\frac{1}{Pr} (1+R)\theta'' + f\theta' + Nb\theta'\phi' + Nt\theta'^2 + Ec f'^2 + \frac{(n-1)}{2} Ec We^2 f''^4 + \frac{2}{m+1} M^2 Ec f'^2 + \frac{Q}{\rho_m} \theta + Du\theta'' = 0, \quad (14)$$

$$\phi'' + Sc f\phi' + \left(\frac{Nt}{Nb} + Sc S_r \right) \theta'' - Kr Sc \phi' = 0. \quad (15)$$

Here β_T, β_C are proportional to x^{-3} , $\beta_T = N x^{-3}$ and $\beta_C = N_1 x^{-3}$ [20].

Corresponding boundary conditions:-

$$f = F_w, \quad f' = 1 + \zeta_p f'', \quad \theta' = -Bi(1 - \theta), \quad \phi = 1 \quad \text{at } \eta = 0. \quad (16)$$

$$f' = 0, \quad \theta = 0, \quad \phi = 0 \quad \text{as } \eta \rightarrow \infty.$$

Where

$$F_w = -\frac{v_w}{\sqrt{\frac{a x^{m-1} \nu (m+1)}{2}}} \text{ is the suction/injection parameter,}$$

$$\zeta_p = l \sqrt{\frac{a(m+1)}{2\nu}} x^{m-1} \text{ is the slip parameter for liquid, and}$$

$$\frac{\beta l}{\sqrt{Re_x}} = \frac{hx}{k} \sqrt{\frac{2}{m+1}} \quad (\text{Surface convection parameter or reduced Biot number}).$$

Where

$$P_{mx} = \frac{x^{m-1}(m+1)}{2}$$

This parameter obliges our equations to be solved locally. Redefining F_w , ζ_p based on the non-linear P_{mx} yields an independent f_w , ζ from x and m as follows [21]:

$$F_w = \frac{f_w}{\sqrt{P_{mx}}}, \quad \zeta_p = \zeta \sqrt{P_{mx}} \quad (17)$$

Physical quantities of interest for present study are:-

$$C_f = \frac{\tau_w}{\rho u_w^2} = \frac{\mu_f}{\rho u_w^2} \left[\frac{\partial u}{\partial y} + \frac{(n-1)\Gamma^2}{2} \left(\frac{\partial u}{\partial y} \right)^3 \right]_{y=0} \quad (18)$$

$$C_f = \sqrt{\frac{1}{2(m+1)}} Re_x^{-1/2} \left\{ f''(0) + \frac{(n-1)We^2}{2} f''^2(0) \right\} \quad (19)$$

$$Nu = \frac{-x}{T_w - T_\infty} \frac{\partial T}{\partial y} \Big|_{y=0} \quad , \quad Sh = \frac{-x}{c_w - c_\infty} \frac{\partial c}{\partial y} \Big|_{y=0} \quad (20)$$

Or by introducing the transformations (12), we get

$$Nu = -\sqrt{\frac{m+1}{2}} Re_x^{1/2} \theta'(0) \quad , \quad Sh = -\sqrt{\frac{m+1}{2}} Re_x^{1/2} \phi'(0) \quad (21)$$

RESULTS AND DISCUSSIONS

The problem of non-Newtonian nanofluid through porous medium with heat and mass transfer is discussed and the system of nonlinear partial differential equations describing this motion is solved numerically. The effects of the Physical parameters of the problem on the obtained solutions are discussed numerically and cleared graphically through a set of figures (2-12). Also, figures a,b,c and d and table (***) illustrated the comparison for special cases of our work.

To save the space of this manuscript we most of figures which describe the effects of parameters are excluded and they are available under your request.

Figure (2) illustrated the effect of non-linear stretching parameter m on the velocity distribution $f(\eta)$, it is observed that an increase of m leads to decrease the velocity field, while the increasing values of

Weissenberg number We enhances the velocity, this because, rising values of the power-law index n helps to reduce the resistive force. The effect of injection parameter f_w on the velocity is to increase it close to the surface of the sheet, this appear through the figure (3). Also, the velocity reduces with the increase of the slip parameter ζ and then, decreases asymptotically to zero at the edge of the boundary layer, this is clear in figure (4). The relation between the velocity and the magnetic field parameter M is plotted, and it is shown that when the values of M rising the velocity depreciates, this due to the fact that the increasing of M creates a drag force and develop the Lorentz force which reduces the motion. The effect of heat generation Q on the velocity is discussed and it is seen that when Q increases the velocity increases. Also, the effect of Prandtl number Pr , Schmidt number Sc , thermophoresis parameter Nt , Forchheimer number Fs are to increases the velocity field. It is observed also ,

that the velocity increases with increasing the Darcy number Da , this due to when Da increases the porosity of the medium increases, then the fluid flow increases.

The effects of the physical parameters on the temperature θ are illustrated through some figures. Figure (5) shows that temperature increases with the increase of the magnetic parameter M . This due to that the nano fluid contains nano size particles whose motion is affected by the magnetic field, and these particles act as energy carrier the fluid, this causing the increasing in nano temperature. The temperature increases with ζ , while it decreases with f_w . Also, the temperature increases with the increasing of thermal and solutal buoyancy parameters the increasing of Q enhances the temperature but it decreases when the radiation R increases it is observed also that the temperature increases with increasing of Brownian motion parameter Nb . Also, when the Diffusion-thermo parameter Du increases the temperature is increasing, this due to Du causes an increase in the thermal boundary layer thickness. The effect of the thermal buoyancy parameter λ on θ are discussed and shown through figure (6). It is observed that θ decreases when λ increases. The effect of the physical parameter on the nanoparticles concentration ϕ are discussed also,. It is seen from figure (7) that the concentration increases as the radiation R increases. Figure (8) illustrates the relation between ϕ and Nt its clear that ϕ decreases as the thermophoresis parameter Nt increases. Also, we noticed that ϕ decreases when ζ , Q , Dm , chemical reaction Kr , Soret number Sr increases, while it increases when the injection parameter f_w and Prandtl number Pr increase.

The effect of solutal buoyancy parameter δ on the skin friction C_f is to decreases it, this appear through the figure (9). The skin friction increases with increasing both of Q , Pr , Sr and Du . The effect of Prandtl number Pr on C_f is illustrated through figure (10). The effects of parameters on Nusselt number Nu

are illustrated and its observed that Nu decreases with increasing both of, δ , Q , Pr , Sr and Du . Figure (11) shows the relation between Nu and Du . At last the effects of these parameters on Sherwood number Sh are illustrated. It is found that the Sherwood Sh increases with increasing both of, δ , Q , Pr , Sr and Du . Figure (12) illustrates the relation between Sh and Du .

CONCLUSION

In our work, we were interested to discuss the Dufour, Soret, chemical reaction, thermal radiation, heat generation; viscous and ohmic dissipation effects on the heat and mass transfer of an electrically conducting Carreau nanofluid flow past an infinite vertical heated permeable stretching sheet with convective boundary conditions. A uniform transverse magnetic field affects the flow in the presence of Brownian motion and thermophoresis. We reduced the governing boundary layer equations to ordinary differential equations, and used Runge-Kutta method with shooting technique to solve the resulting equation numerically. We have systematically examined the influence of various governing parameters on the velocity, temperature, concentration distributions as well as skin-friction coefficient, heat and mass transfer rates. The following concluded remarks can be drawn from the present numerical investigation:

- Velocity accelerates with an increase in Weissenberg number We , heat generation parameter Q , Prandtl number Pr , Schmidt number Sc , thermophoresis parameter Nt , the non-linear stretching parameter m , local Forchheimer number Fs and local Darcy number Da and decelerates with an increase in slip parameter ζ and magnetic field M .
- Temperature rises with an increase in the slip parameter ζ , magnetic field parameter M , heat generation parameter Q , Brownian motion parameter Nb , thermophoresis parameter Nt , Dufour number Du and it is fall with an increase in the thermal

buoyancy parameter λ , injection parameter f_w , radiation parameter R and Darcy number Da .

- There is an increase in particles concentration with increasing in the injection parameter f_w or radiation parameter R , whereas there is a decrease in the concentration with the increase in the value of the slip parameter ζ , heat generation parameter Q , Prandtl number Pr , thermophoresis parameter Nt , chemical reaction Kr and Soret number Sr .
- There is an increase in Skin friction coefficient as a result of increasing the heat generation parameter Q , Prandtl number Pr , Soret number Sr , Dufour number Du whereas there a decrease following an increase in the solutal buoyancy parameter δ .
- There is a fall in heat transfer rate as a result of increasing the solutal buoyancy parameter, heat generation parameter, Prandtl number, Soret number or Dufour number.
- There is an increase in mass transfer as a result of increasing the solutal buoyancy parameter or heat generation parameter or Prandtl number or Soret number or Dufour number.

Applications

1. A great number of researchers have been interested in the problems of free convective and heat transfer flows through a porous medium under the influence of a magnetic field due to their applications in transportation cooling of re-entry vehicles and rocket boosters, cross-hatching on ablative surfaces and film vaporization in combustion chambers.
2. There are several engineering and geophysical applications of flow through a porous medium e.g filtration and purification process in chemical engineering, studying the underground water resources in agriculture engineering and studying the movement of natural gas,

oil and water through the oil reservoirs in petroleum technology.

3. It is greatly important to analyze non-Newtonian fluid flows generated by a stretching sheet in several manufacturing processes such as extrusion of molten polymers through a slit die for the production of plastic sheets, processing of food stuffs, paper production, and wire and fiber coating.

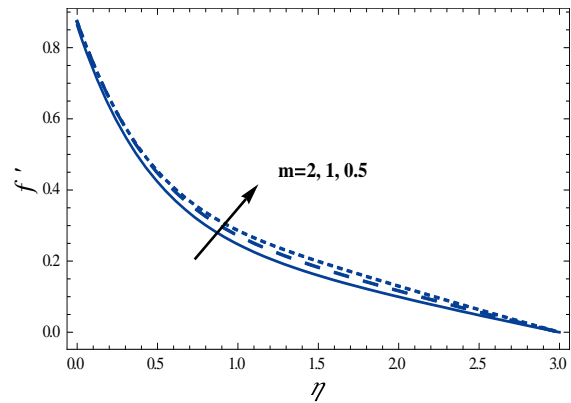


Figure (2) The velocity distribution is plotted against η for different values of m with $n = 2$, $We = 0.3$, $M = 1$, $\lambda = 1$, $\delta = 1$, $Q = 0.5$, $R = 0.5$, $Pr = 0.7$, $Nb = 0.5$, $Sc = 1$, $Nt = 0.5$, $Ec = 0.1$, $Re = 0.3$, $Kr = 0.2$, $Sr = 1$, $Du = 0.05$, $Fs = 0.1$, $Da = 0.5$, $f_w = 0.1$, $\zeta = 0.1$ and $Bi = 0.5$.

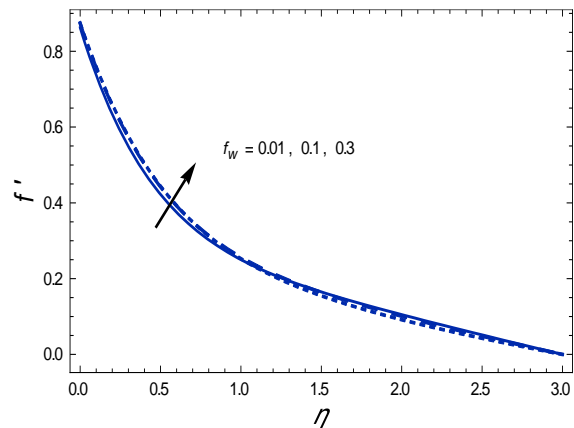


Figure (3) The velocity distribution is plotted against η for different values of f_w with $n = 2$, $m = 2$, $M = 1$, $\lambda = 1$, $\delta = 1$, $Q = 0.5$, $R = 0.5$, $Pr = 0.7$, $Nb = 0.5$, $Sc = 1$, $Nt = 0.5$, $Ec = 0.1$, $Re = 0.3$, $Kr = 0.2$, $Sr = 1$, $Du = 0.05$, $Fs = 0.1$, $Da = 0.5$, $We = 0.1$, $\zeta = 0.1$ and $Bi = 0.5$.

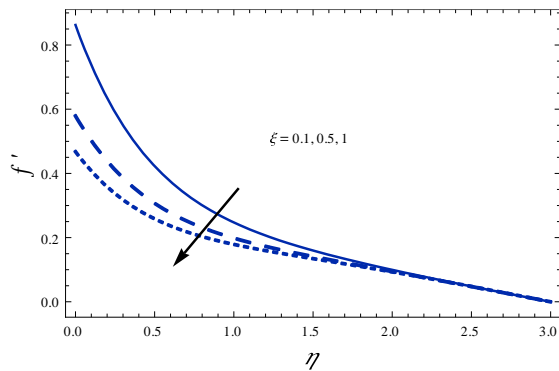


Figure (4) The velocity distribution is plotted against η for different values of ζ with $n = 2, m = 2, M = 1, \lambda = 1, \delta = 1, Q = 0.5, R = 0.5, Pr = 0.7, Nb = 0.5, Sc = 1, Nt = 0.5, Ec = 0.1, Re = 0.3, Kr = 0.2, Sr = 1, Du = 0.05, Fs = 0.1, Da = 0.5, fw = 0.1, We = 0.3$ and $Bi = 0.5$.

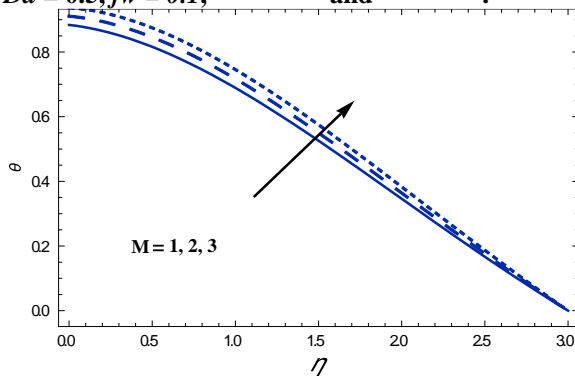


Figure (5) The temperature distribution is plotted against η for different values of M with $n = 2, m = 2, \zeta = 0.1, \lambda = 1, \delta = 1, Q = 0.5, R = 0.5, Pr = 0.7, Nb = 0.5, Sc = 1, Nt = 0.5, Ec = 0.1, Re = 0.3, Kr = 0.2, Sr = 1, Du = 0.05, Fs = 0.1, Da = 0.5, fw = 0.1, We = 0.3$ and $Bi = 0.5$.

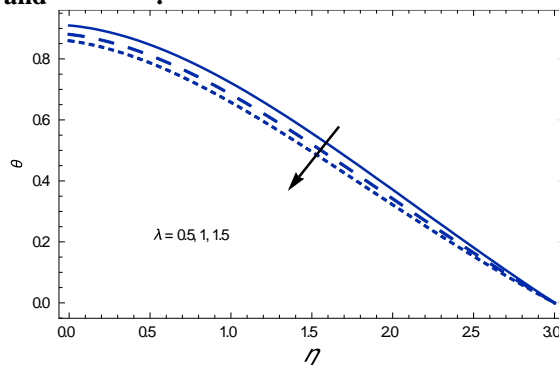


Figure (6) The temperature distribution is plotted against η for different values of λ with $n = 2, m = 2, M = 1, \zeta = 0.1, \delta = 1, Q = 0.5, R = 0.5, Pr = 0.7, Nb = 0.5, Sc = 1, Nt = 0.5, Ec = 0.1, Re = 0.3, Kr = 0.2, Sr = 1, Du = 0.05, Fs = 0.1, Da = 0.5, fw = 0.1, We = 0.3$ and $Bi = 0.5$.

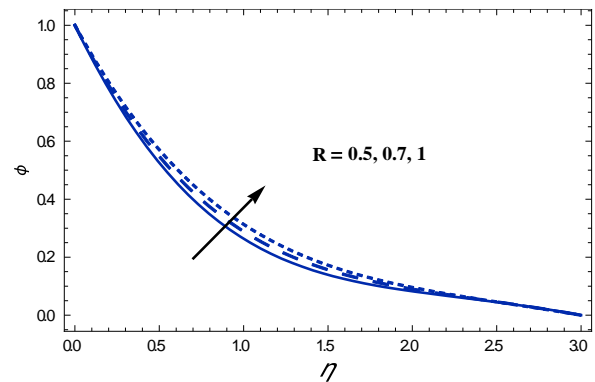


Figure (7) The nanoparticles concentration distribution is plotted against η for different values of R with $n = 2, m = 2, M = 1, \lambda = 1, \delta = 1, Q = 0.5, fw = 0.1, Pr = 0.7, Nb = 0.5, Sc = 1, Nt = 0.5, Ec = 0.1, Re = 0.3, Kr = 0.2, Sr = 1, Du = 0.05, Fs = 0.1, Da = 0.5, \zeta = 0.1, We = 0.3$ and $Bi = 0.5$.

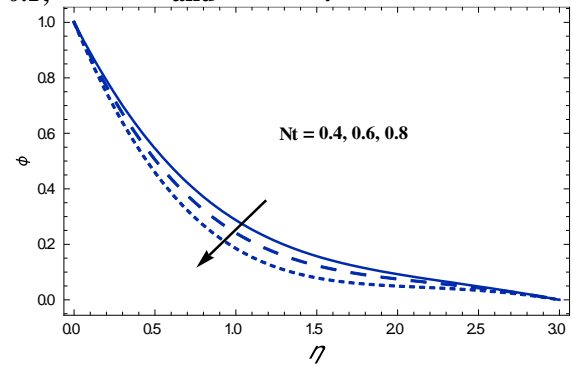


Figure (8) The nanoparticles concentration distribution is plotted against η for different values of Nt with $n = 2, m = 2, M = 1, \lambda = 1, \delta = 1, Q = 0.5, R = 0.5, Pr = 0.7, Nb = 0.5, Sc = 1, fw = 0.1, Ec = 0.1, Re = 0.3, Kr = 0.2, Sr = 1, Du = 0.05, Fs = 0.1, Da = 0.5, \zeta = 0.1, We = 0.3$ and $Bi = 0.5$.

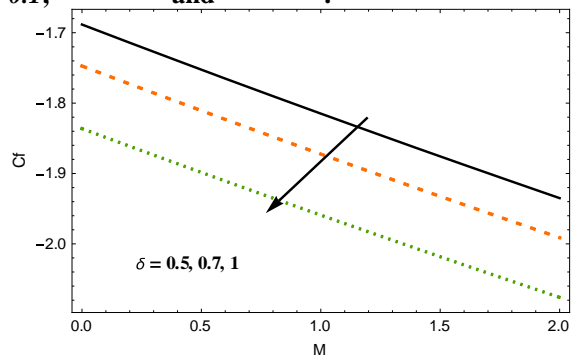


Figure (9) The skin friction distribution is plotted against η for different values of δ with $n = 2, m = 2, M = 1, \lambda = 1, \zeta = 0.1, Q = 0.5, R = 0.5, Pr = 0.7, Nb = 0.5, Sc = 1, Nt = 0.5, Ec = 0.1, Re = 0.3, Kr = 0.2, Sr = 1, Du = 0.05, Fs = 0.1, Da = 0.5, fw = 0.1, We = 0.3$ and $Bi = 0.5$.

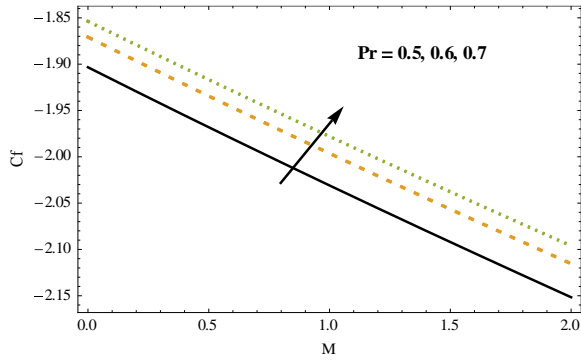


Figure (10) The skin friction distribution is plotted against η for different values of Pr with $n = 2, m = 2, M = 1, \lambda = 1, \zeta = 0.1, \delta = 0.1, R = 0.5, Q = 0.5, Nb = 0.5, Sc = 1, Nt = 0.5, Ec = 0.1, Re = 0.3, Kr = 0.2, Sr = 1, Du = 0.05, Fs = 0.1, Da = 0.5, fw = 0.1, We = 0.3$ and $Bi = 0.5$.

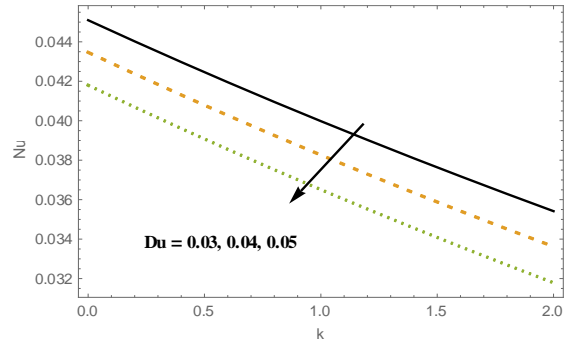


Figure (11) The Nusselt number distribution is plotted against η for different values of Du with $n = 2, m = 2, M = 1, \lambda = 1, \zeta = 0.1, Q = 0.5, R = 0.5, Pr = 0.7, Nb = 0.5, Sc = 1, Nt = 0.5, Ec = 0.1, Re = 0.3, Kr = 0.2, Sr = 1, \delta = 0.1, Fs = 0.1, Da = 0.5, fw = 0.1, We = 0.3$ and $Bi = 0.5$.

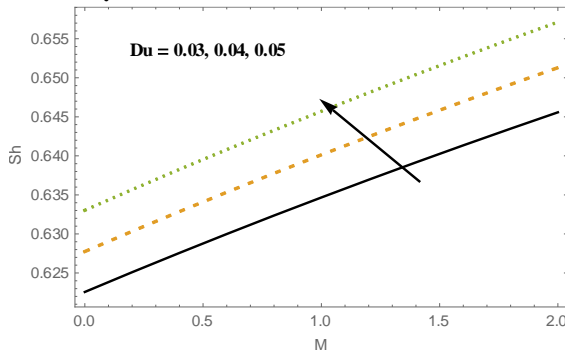


Figure (12) The Sherwood number distribution is plotted against η for different values of Du with $n = 2, m = 2, M = 1, \lambda = 1, \zeta = 0.1, Q = 0.5, R = 0.5, Pr = 0.7, Nb = 0.5, Sc = 1, Nt = 0.5, Ec = 0.1, Re = 0.3, Kr = 0.2, Sr = 1, \delta = 0.1, Fs = 0.1, Da = 0.5, fw = 0.1, We = 0.3$ and $Bi = 0.5$.

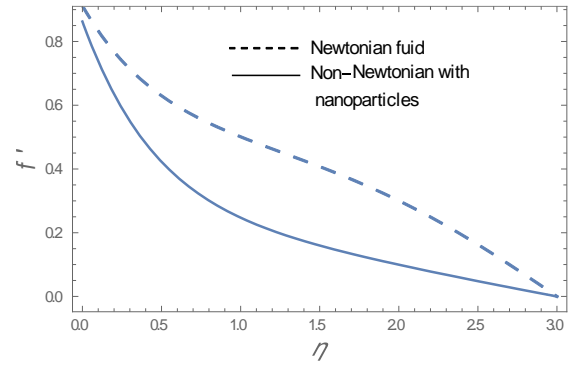


Fig.(a) The velocity distribution is plotted against η in the case of $We = 0, Nb = 0, Nt = 0$ and $F_w = 0$

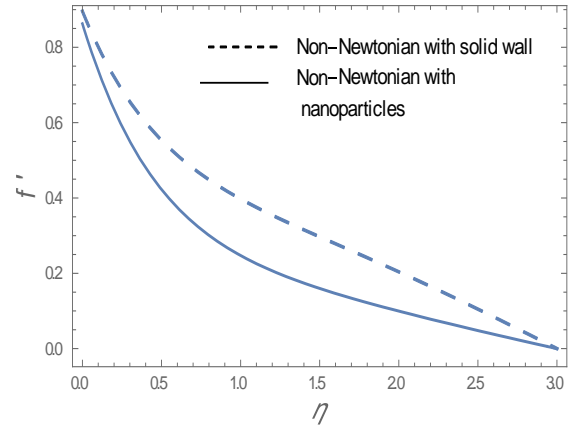


Fig.(b) The velocity distribution is plotted against η in the case of the solid wall $F_w = 0$

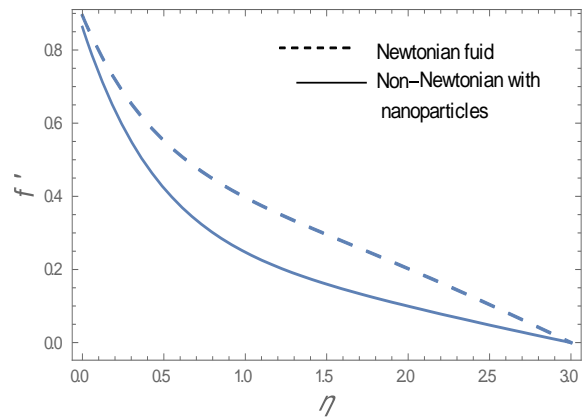


Fig.(c) The velocity distribution is plotted against η in the case of the Newtonian fluid $We = 0, Nb = 0, Nt = 0$

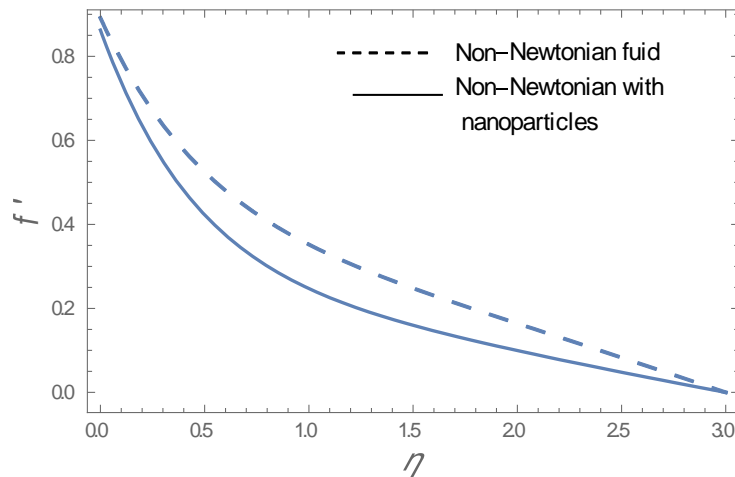


Fig.(d) The velocity distribution is plotted against η in the case of nanoparticles
 $Nb = 0$, $Nt = 0$

Table (**) illustrated the comparison of the values the velocity, the temperature, the concentration of the fluid when $n = 2, m = 2, M = 1, \lambda = 1, \delta = 1, Q = 0.5, R = 0.5, Pr = 0.7, Sc = 1, Ec = 0.1, Re = 0.3, Kr = 0.2, Sr = 1, Du = 0.05, Fs = 0.1, Da = 0.5, \zeta = 0.1$ and $Bi = 0.5$. in general case and for special cases the following. solid wall $F_w = 0$, in the absence of nanoparticles $Nb = 0, Nt = 0$, in ordinary Newtonian fluid $We = 0$

Nb	Nt	F_w	We	$f'(0)$	$\theta(0)$	$\phi(0)$
0.5	0.5	0.1	0.3	0.159742	0.525715	0.139238
0	0	0.1	0.3	0.119236	0.423857	0.230237
0.5	0	0.1	0.3	0.133907	0.474678	0.212135
0	0.5	0.1	0.3	0.131192	0.475016	0.207844
0.5	0.5	0	0.3	0.165613	0.56769	0.119912

REFERENCES

[1] I. C. Bang and S. H. Chang. "Boiling heat transfer performance phenomena of Al_2O_3 - water nano-fluids from a plain surface in a pool" *International Journal of Heat and Mass Transfer* ,Vol. 48(12), PP. 24007-2419 (2005).

[2] K. S. Suganthi and K. S. Rajan. "Temperature induced changes in ZnO water nanofluid: Zeta potential size distribution and viscosity profiles" *International Journal of Heat and Mass Transfer*, Vol. 55, PP. 7969-7980 (2012).

[3] A. V. Kuznetsov."Nanofluid bioconvection in water-based suspensions containing nanoparticles and oxytactic microorganism: oscillatory instability" *Nanoscale Research Letter*, Vol. 6, PP. 100 (2011).

[4] Alam. M. S and Rahman. M. M." Dufour and Soret effects on MHD free convective heat and mass transfer flow past a vertical flat plate embedded in a porous medium" *J. Naval Architecture and Marine Engng.*, Vol.2(1), PP. 55-65 (2005).

[5] H. Masuda, A. Ebata, K. Teramae and N. Hishinuma. "Alteration of Thermal Conductivity and Viscosity of Liquid by Dispersing Ultra-Fine Particles" *Netsu Bussei*, Vol. 7, PP. 227-233 (1993).

[6] El-Dabe, Nabil, Abeer A. Shaaban, Mohamed Y. Abou-Zeid, and Hemat A. Ali. "Magnetohydrodynamic non-Newtonian nanofluid flow over a stretching sheet through a non-Darcy porous medium with radiation and chemical reaction." *Journal of Computational and Theoretical Nanoscience* 12, no. 12: 5363-5371 (2015).

- [7] Awais M, Hayat T, Aamir A, Irum S "Velocity, thermal and concentration slip effects on a magneto-hydrodynamic nanofluid flow." *Alex Eng J* 55:2107–2114 (2016).
- [8] El-dabe, Nabil TM, Mohamed Y. Abou-zeid, and Yasmeen M. Younis. "Magneto-hydrodynamic peristaltic flow of Jeffrey nanofluid with heat transfer through a porous medium in a vertical tube." *Applied Mathematics & Information Sciences* 11, no. 4 : 1097-1103 (2017).
- [9] B. C. Sakiadis, "Boundary layer behavior on continuous solid flat surfaces," *American Institute of Chemical Engineers Journal*, Vol. 7, PP 26-28 (1961)
- [10] F. K. Tsou, E. M. Sparrow and R. J. Goldstein. "Flow and heat transfer in the boundary layer on a continuous moving surface" *International Journal of Heat and Mass Transfer*, Vol. 10, PP. 219-235 (1967)
- [11] L. E. Erickson L. T. Fan and V. G. Fox "Heat and Mass transfer in the laminar boundary layer flow of a moving flat surface with constant surface velocity and temperature focusing on the effects of suction/injection. *Industrial & Engineering Chemistry Fundamentals*, Vol. 5, PP. 19-25 (1966)
- [12] I. C. Liu "A note on heat and mass transfer for a hydromagnetic flow over a stretching sheet" *International Communications in Heat and Mass Transfer*, Vol. 8, PP. 1075-1084 (2005)
- [13] M. A. A. Hammad and M. Ferdows "Similarity solutions to viscous flow and heat transfer of nanofluid over nonlinearly stretching sheet" *Applied Mathematics (English Edition)*, Vol. 7, PP. 923-930 (2011)
- [14] F. M. Ali, R. Nazar, N. M. Arifin and I. Pop "MHD stagnation-point flow and heat transfer to wards stretching sheet with induced magnetic field" *Applied Mathematics (English Edition)*, Vol. 4, PP. 409-418 (2011)
- [15] N. Eldabe, A. Elsaka, A. Radwan, M. Eltaweel " Effect of chemical reaction and heat radiation on the MHD flow of viscoelastic fluid through a porous medium over a horizontal stretching flat plate " *J. of American Science*, Vol. 9, pp. 126-136 (2010)
- [16] N. Eldabe, G. Saddeek, A. El- Sayed, " Heat and mass transfer of MHD unsteady Maxwell fluid flow through porous medium past a porous flat plate" *J. Egypt. Math. Soc.*, Vol. 2, pp. 189-200 (2005)
- [17] Khan WA, Pop I "Boundary layer flow of a nanofluid past a stretching sheet." *Int J Heat Mass Transf* 53:2477–2483 (2010).
- [18] Ganga B, Ansari SMY, Vishnu Ganesh N, Abdul Hakeem AK. "MHD radiative boundary layer flow of nanofluid past a vertical plate with internal heat generation/absorption, viscous and ohmic dissipation effects." *J Niger Math Soc* 34:181–194 (2015).
- [19] Abou-zeid, Mohamed. "Magneto-hydrodynamic boundary layer heat transfer to a stretching sheet including viscous dissipation and internal heat generation in a porous medium." *J. of Porous Media* 14, no. 11, pp.1007-1018 (2011).
- [20] O. D. Makinde and P. O. Olanrewaju, *J. Fluids Eng. Trans. ASME*, vol. 132:044502, pp. 1 – 4 (2010).
- [21] M. H. Yazdi, S. Abdullah, I. Hashim, K. Sopian. "Slip MHD liquid flow and heat transfer over non-linear permeable stretching surface with chemical reaction" *Int. J. Heat Mass Transfer*, Vol. 54, PP.3214-3225(2011).

المخلص العربي

التأثير الإشعاعي على تدفق مانع نانو غير نيوتوني ممغنط يتبع نموذج كاريو مع الانتقال الحرارى و الكتلى على سطح مطاطى فى وجود قوى مختلفة.

أ.د/ نبيل توفيق محمد الضبع (استاذ بقسم الرياضيات بكلية التربية جامعة عين شمس)

Eng_mohamed_nabil125@hotmail.com

أ.م.د/كوثر أحمد كامل (أستاذ مساعد فى الرياضيات التطبيقية كلية العلوم (بنات) – جامعة الأزهر)

hesho_9000@yahoo.com

osama_96348@yahoo.com

د/ حميدة محمد شوقى (أستاذ مساعد فى الرياضيات التطبيقية كلية العلوم (بنات) – جامعة الأزهر)

د / عصمت عبد الحميد عبد العزيز متولى (باحثة - كلية العلوم (بنات) – جامعة الأزهر)

esmat.abdelazeez@yahoo.com

تم فيه دراسة تدفق الحركة الأنزلاقية الجدارية لمائع نانو غير نيوتوني ممغنط يتبع نموذج "Carreau" على سطح رأسى مطاطى نفاذ ساخن خلال وسط مسامى غير دارسى مع الانتقال الحرارى و الكتلى فى وجود اشعاعى و توليد حرارى و تفاعل كيميائى مع الأخذ فى الاعتبار تأثير التشتت الناتج عن اللزوجة و المغناطيسية وقد تم تمثيل هذه الدراسة رياضيا من خلال مجموعة من المعادلات التفاضلية الجزئية غير الخطية التى تمثل كمية الحركة و الطاقة و التركيزو التى تم تحويلها الى معادلات تفاضلية عادية بإستخدام تحويلات تماثلية. و بإستخدام شروط حدية مناسبة أمكن إيجاد الحلول العددية لهذه المعادلات بإستخدام طريقة رنج- كوتا (Runge-Kutta) من الرتبة الرابعة مع تكنولوجيا التنشين (Shooting technique) مع العرض البيانى بإستخدام برنامج الماثيماتيك و ذلك عند قيم مختلفة للبارامترات الفيزيائية الخاصة بالمسألة و بإستعانة بالأشكال البيانية تم توضيح تأثير المعاملات الفيزيائية المختلفة على مجالات السرعة و الحرارة و التركيزو كذلك الاحتكاك السطحى و معدل الانتقال الحرارى و الكتلى.